Effects of Framework Flexibility on the Adsorption and Diffusion of Aromatics in MFI-Type Zeolites

Caro-Ortiz, Sebastián; Zuidema, Erik; Rigutto, Marcello; Dubbeldam, David; Vlugt, Thijs J.H.

DOI
10.1021/acs.jpcc.0c08054

Publication date
2020

Document Version
Final published version

Published in
Journal of Physical Chemistry C

Citation (APA)
Caro-Ortiz, S., Zuidema, E., Rigutto, M., Dubbeldam, D., & Vlugt, T. J. H. (2020). Effects of Framework Flexibility on the Adsorption and Diffusion of Aromatics in MFI-Type Zeolites. *Journal of Physical Chemistry C*, *124*(44), 24488-24499. https://doi.org/10.1021/acs.jpcc.0c08054

THE JOURNAL OF PHYSICAL CHEMISTRY C

pubs.acs.org/JPCC Article

Effects of Framework Flexibility on the Adsorption and Diffusion of Aromatics in MFI-Type Zeolites

Sebastián Caro-Ortiz, Erik Zuidema, Marcello Rigutto, David Dubbeldam, and Thijs J. H. Vlugt*

Cite This: *J. Phys. Chem. C* 2020, 124, 24488−24499 Read Online

ABSTRACT: We systematically study how the degree of framework flexibility affects the adsorption and diffusion of aromatics in MFI-type zeolites as computed by Monte Carlo simulations. It is observed that as the framework is more flexible, the zeolite structure is inherently changed. We have found that framework flexibility has a significant effect on the adsorption of aromatics in MFI-type zeolites, especially at high pressure. Framework flexibility allows the zeolite framework to accommodate to the presence of guest aromatic molecules. For very flexible zeolite frameworks, loadings up to two times larger than that in a rigid zeolite framework are obtained at a given pressure. We assessed the "flexible snapshot" method, which captures framework flexibility using independent snapshots of the framework. We have found that this method only works well when the loadings are low. This suggests that the effect of the guest molecules on the zeolite framework is important. Framework flexibility lowers the free-energy barriers between low energy states, increasing the rate of diffusion of aromatics in the straight channel of MFI-type zeolites for many orders of magnitude compared to a rigid zeolite framework. The simulations show that framework flexibility should not be neglected and that it significantly affects the diffusion and adsorption properties of aromatics in an MFI-type zeolite.

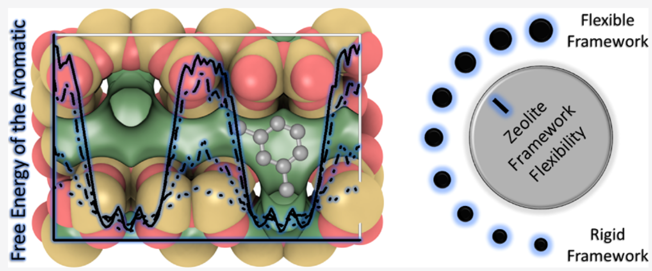

1. INTRODUCTION

The diversity of the application of zeolites is wide and ranges from being used as a catalyst for the petrochemical industry[1] to builder for laundry powders,[2] odor control agents,[3] and many other applications.[4−8] Many petrochemical processes strongly rely on the interaction and kinetic behavior of hydrocarbons inside a zeolite.[9−13] For example, xylene molecules diffusing along the zeolite pores can undergo isomerization, disproportionation, and transalkylation reactions.[14] Thus, knowledge of the adsorption and diffusion behavior of hydrocarbons in the pores of zeolites is important for the understanding of the catalytic activity of the zeolite.[15−18]

The adsorption and diffusion of aromatics in MFI-type zeolites has been reported by several experimental studies.[19−36] The interaction of an aromatic molecule within a zeolite framework is a complex process.[37] Factors such as molecules filling a new adsorption site,[38,39] structural changes due to the number of adsorbed molecules,[19,40,41] or structural changes due to a change of temperature[42,43] may result in an inflection point in the adsorption isotherm. Talu et al.[19] reported that with increasing temperature, the isotherm shape for benzene, toluene, and *p*-xylene changes from type IV to type I. The combination of such factors also leads to different phases of MFI-type zeolite structures. The all-silica form of the MFI-type zeolite is known to show a monoclinic or orthorhombic structure depending on the temperature and loadings.[20,44] van Koningsveld et al.[45] identified three structures of the *p*-xylene/silicalite system: Mono (monoclinic), Ortho (orthorhombic), and Para (also orthorhombic).

The adsorption and diffusion of aromatics in MFI-type zeolites has also been studied by molecular simulations.[17] Commonly, Monte Carlo (MC) simulations in the grand-canonical ensemble are used to compute sorbate loadings as a function of temperature and pressure in a zeolite framework.[46−48] Several studies where MC is used to study the adsorption of aromatics in MFI-type zeolites can be found in the literature.[37,49−62] Zeolites are commonly considered as very rigid structures as their atomic bonds and angles are highly constrained.[63,64] Computer simulations of the adsorption of hydrocarbons in zeolites are typically performed assuming that the zeolite framework taken from crystallographic data is a rigid structure.[46,65,66] Nevertheless, Clark and Snurr[67] showed that the computed adsorption isotherms are sensitive to small differences in the atom positions of the zeolite. Framework flexibility is observed to play a role only if the adsorbate fits tightly in the zeolite pore.[67] Vlugt et al.[65,68]

Received: September 3, 2020
Revised: October 5, 2020
Published: October 22, 2020

https://dx.doi.org/10.1021/acs.jpcc.0c08054
J. Phys. Chem. C 2020, 124, 24488−24499

reported the effect of framework flexibility in the adsorption of *n*-alkanes and cycloalkanes in MFI-type zeolites. It was found that for molecules with an inflection behavior in the isotherm, the influence of the flexibility seems to be larger than that for molecules without such inflection. Caro-Ortiz et al.[37] showed that the use of force fields for framework flexibility significantly affects the adsorption isotherm of xylene isomers and ethylbenzene in MFI-type zeolites. Such effect is related to intrinsic changes of the zeolite structure caused by the intraframework interactions of the force field for framework flexibility. Framework flexibility has also been studied in other porous materials such as metal−organic frameworks (MOFs) and zeolitic imidazolate frameworks.[69−75] A recent review of the development of force fields for framework flexibility in MOFs by Heinen and Dubbeldam[76] shows that there is an urgent need for efficient sampling schemes that capture stimuli-driven phase transitions for these materials. This limits the predictive capacity of existing force fields for framework flexibility in MOFs.[76]

Molecular dynamic studies have shown that accounting for framework flexibility considerably affects the diffusion coefficient of aromatics in zeolites.[14] Forester et al.[77] reported that framework flexibility changes the diffusivity of aromatics in zeolites by an order of magnitude. Toda et al.[14] assessed the performance of several force fields for framework flexibility by computing diffusion coefficients of *p*-xylene and *o*-xylene in 10-ring zeolites. It is observed that force fields for framework flexibility distort the structure and that the size and shape of the 10-rings act as bottlenecks for the diffusion.[14] Kolokathis et al.[78] computed self-diffusion coefficients of *p*-xylene and benzene in silicalite-1 based on transition state theory (TST). It is found that *p*-xylene diffuses roughly 100 times faster than benzene when adsorbed at low occupancy in silicalite.

If the diffusion coefficient of a molecule in a zeolite framework is sufficiently high, molecular dynamic simulations can be directly used.[17] Processes such as the separation of aromatic isomer mixtures in zeolites show self-diffusivity coefficients lower than 10^{-12} m^2 s^{-1}.[79] As such, the diffusion behavior may occur outside the time scales accessible to molecular dynamics simulations.[80] The free-energy landscape of molecules within the pores of a zeolite shows the mobility of the molecules inside the zeolite and can be used in a more quantitative investigation of product shape selectivity of zeolite catalysts.[81] Low diffusion coefficients are observed when the molecules are trapped in low free-energy sites in the zeolite framework and sporadically hop from one low energy site to another.[17] TST methods can be used to estimate the diffusion coefficients in porous materials at slow diffusion time scales[82−84] using the free-energy landscape.[85] Such methods have been used for the estimation of diffusion coefficients of aromatics in MFI-type zeolites.[77,78,86−88] Caro-Ortiz et al.[37] showed that force fields for framework flexibility produce a zeolite structure that vibrates around a new equilibrium configuration with limited capacity to accommodate bulky guest molecules. To the best of our knowledge, molecular simulation studies where the effect of framework flexibility on the adsorption and diffusion of aromatics in zeolites is systematically studied are not available.

This article explores how the variation of framework flexibility in a model affects the adsorption and diffusion of aromatic hydrocarbons in MFI-type zeolites. Force fields for framework flexibility that include intraframework Lennard-Jones (LJ) and electrostatic interactions induce small but important changes in the atom positions of the zeolite, affecting the adsorption isotherm.[37] The Demontis model[89] consists of modeling zeolite framework flexibility by a bond-stretching potential for the Si−O bond and a bond-stretching potential for oxygen atoms linked by a silicon atom, not including intraframework LJ and electrostatic interactions. The effect of framework flexibility on the adsorption and diffusion of C_8 aromatics in MFI-type zeolites is studied using a Demontis-like model in which the spring constants of such bond-stretching parameters are varied. MC simulations are used to compute adsorption of ethylbenzene and xylene isomers in an MFI-type zeolite structure when framework flexibility is varied. Also, free-energy profiles are used to obtain the self-diffusion coefficients of aromatics in the straight channel of the zeolite.

This article aims to study how variations of framework flexibility change the MFI-type zeolite framework and influence the interactions with guest molecules. The "flexible snapshot" method has been developed by Sholl et al.[90−92] to capture the effect of framework flexibility on adsorption in nanoporous materials. In this method, snapshots are obtained using fully flexible MD simulation of an empty framework and have been used to study the selectivities of C_8 aromatics in multiple MOFs.[92] In this work, the "flexible snapshot" method is used to see how the empty zeolite structure changes due to framework flexibility. The potential of this method to describe adsorption at high pressures is briefly assessed. The simulation procedure is explained in Section 2. The computed Henry coefficients, diffusion coefficients, and adsorption isotherms of C_8 aromatics in an MFI-type zeolite are reported and discussed in Section 3. It is shown that framework flexibility induces small but important changes in the atom positions of the zeolite and hence in the adsorption isotherm and the diffusion coefficient of aromatics in MFI-type zeolites. The concluding remarks regarding the effect of the framework flexibility on the interaction of aromatics within MFI-type zeolites are discussed in Section 4.

2. METHODS

The adsorption computations are performed using the Continuous Fractional Component Monte Carlo (CFCMC)[93,94] algorithm in the grand-canonical ensemble. RASPA software[95,96] is used for all simulations. Periodic boundary conditions are applied to a simulation box consisting of 2 × 2 × 3 unit cells of the MFI-type zeolite Ortho structure described by van Koningsveld et al.[97] A cut off radius of 14 Å is applied for all LJ interactions, and analytic tail corrections are used.[98] The interactions between different atom types are obtained using Lorentz−Berthelot mixing rules.[99] MC simulations are performed in MC cycles. The number of trial moves per cycle equals the number of adsorbed molecules N with a minimum of 20. At each MC cycle, trial moves attempt to rotate, displace, randomly reinsert, and insert/remove adsorbates. In the CFCMC algorithm, the interactions of a fractional molecule are scaled by the λ parameter in the range 0−1 (0 for no interactions with surrounding molecules/framework and 1 for full interaction with surrounding molecules/framework). The so-called λ-trial moves scale the interactions of the fractional molecule via the CFCMC algorithm.[93,94] The simulations use 10^5 MC cycles to initialize the system. The initialization run only allows translation, rotation, insertion/deletion, and reinsertion trial moves. After

https://dx.doi.org/10.1021/acs.jpcc.0c08054
J. Phys. Chem. C 2020, 124, 24488−24499

initialization, a stage of 4×10^5 MC cycles are used to equilibrate the CFCMC biasing factors. All the considered types of trial moves are allowed, and the biasing factors for the λ-trial moves of the CFCMC algorithm are calculated. λ-trial moves are biased to obtain a flat λ probability distribution. The use of this trial move is advantageous as it enables an efficient insertion and deletion of sorbate molecules in the system.[94,100,101] Ensemble averages are obtained in a 5×10^5 MC cycle production stage. The reported errors account for the 95% confidence interval calculated by dividing the production run into five parts and computing the standard deviation. An additional MC trial move is included to simulate a flexible zeolite framework, which attempts to give a random displacement to a randomly selected zeolite atom.[65] *p*-Xylene and benzene adsorption cause volume changes of the MFI-type framework smaller than 0.4%[23,102] at high loadings (4 to 8 molec./u.c.). As such, the volume of the simulation box in this work is kept fixed.

The framework snapshots considered for the "flexible snapshot" method[90−92] are obtained by performing simulations of an empty zeolite structure in the *NVT* ensemble. Random framework atom trial moves are allowed. A 10^5 MC cycle run is performed as initialization. After that, snapshots are produced every 10^4 MC cycles. The average properties for each snapshot are computed and then averaged.

The pore size distribution (PSD) of an MFI-type structure is calculated geometrically with the method reported by Gelb and Gubbins.[103,104] Henry coefficients and free-energy profiles of aromatics in the MFI-type zeolite structure are calculated via the Widom test-particle insertion method.[105] In this method, the average Boltzmann weight of a ghost molecule is calculated. Such ghost molecule perceives the same energy as a real particle. The other molecules in the system (zeolite framework in this case) do not feel the presence of the ghost particle.[106] The simulations are started with 10^5 MC cycles to initialize the system. The initialization run only allows framework atom moves. After that, the Henry coefficient and free-energy landscape are computed in a 10^5 MC cycle production run. The helium void fraction (HVF) is determined using iRASPA visualization software[107] by probing the framework with a non-adsorbing helium molecule using the Widom test-particle insertion method.[105]

Force fields that model the flexibility of the zeolite framework are commonly based on the description of vibrational properties, such as the infrared spectra of the zeolite atoms[108,109] and/or ab initio quantum chemical calculations.[110,111] Several force fields for framework flexibility have been reported in the literature.[63,89,110−117] Such force fields are typically used for the calculations of diffusion of aromatics in MFI-type zeolites by molecular dynamics simulations.[14,118] In this work, the host−host interactions are modeled using a Demontis-like force field. The Demontis model[89,113,114] consists of modeling zeolite framework flexibility by a bond-stretching potential for the Si−O bond and a bond-stretching potential for the oxygen atoms linked by a silicon atom. The bond-stretching potentials U are modeled using the expression: $U(r) = 0.5 \times k \times (r - r_0)^2$, where k is the spring constant and r_0 is the equilibrium bond length. The original values of the spring constants are $k_{O-(Si)-O}/k_B$ = 51,831.61 K Å^{-2} and k_{Si-O}/k_B = 251,778.07 K Å^{-2}. To reduce the number of parameters, the ratio $k = k_{O-(Si)-O} = 0.2 \times k_{Si-O}$ is kept fixed.[65] The original Demontis model[89] uses constant equilibrium bond lengths and angles. The so-called modified form of this model takes the equilibrium bond lengths and bend-angles (in the Urey−Bradley term) directly from the crystallographic structure to which the model is applied.[65] This modification is used in this work, and it is used to avoid large deviations from the experimental crystal structure.[37] When this modification is in use, the minimum energy structure is exactly reproduced when $k \to \infty$[65] or for any value of the spring constant k when $T \to 0$ K.

The interactions between the zeolite and guest hydrocarbons are modeled using the TraPPE-zeo model.[119] In this force field, all oxygen and silicon atoms are modeled with LJ interactions and partial charges. The development of this force field was focused on transferability and variety of zeolite/guest systems.[119] As such, it is fitted to match the experimental adsorption isotherms of *n*-heptane, propane, carbon dioxide, and ethanol in zeolites.

Molecular simulations of aromatics typically use force fields (guest−guest interactions) that model the vapor−liquid equilibrium (VLE) with LJ potentials or a combination of LJ and electrostatic interactions.[120,121] In the case of aromatic species, a common practice in the development of these force fields is to fit the interaction parameters to reproduce the VLE of the pure components[122−128] or by optimizing LJ interactions by a combination of ab initio quantum mechanical calculations and empirical methods.[129−133] In this work, the guest−guest interactions are modeled using the TraPPE-UA[134] force field. The TraPPE-UA is a widely used force field that is designed to reproduce the VLE of alkylbenzenes and *n*-alkanes, among other chemical species. The united atom approach is used by merging a carbon atom and its bonded hydrogen atoms into a single uncharged interaction site representing each CH_x group in the aromatic species. Aromatics are modeled as rigid molecules, except ethylbenzene that includes a torsional potential in the CH_3-CH_2-CH bend angle. Electrostatic interactions (guest−guest, guest−host, and host−host) are not considered in this work, as electrostatic interactions are not a part of the TraPPE-UA force field for xylenes[134] Framework flexibility is also important for adsorption and diffusion in zeolites containing extra-framework cations. Studies exploring the effect of framework flexibility in such systems require models that include electrostatic interactions for the zeolite atoms and guest molecules. However, models for framework flexibility that include intraframework electrostatic interactions inherently change the zeolite structure, significantly affecting adsorption.[37] This suggests that to study the effect of framework flexibility in zeolites containing extra-framework cations, strategies different than those used in this work might be needed.

The reader is referred to ref 37 for details about the choice of force fields and the parameters used in this work.

3. RESULTS AND DISCUSSION

The Henry coefficients of ethylbenzene and xylene isomers (as single components) in an MFI-type zeolite at 353 K are computed using the flexible framework model and the "flexible snapshot" method, varying *k*. Five snapshots are used for the "flexible snapshot" method. The computed Henry coefficients as a function of the framework flexibility are shown in Figure 1. It is observed that for all aromatics considered in this study, the "flexible snapshot" method yields the same Henry coefficient as the simulations using a flexible framework.

Figure 1 shows that framework flexibility has a significant influence on the Henry coefficient of aromatics in the MFI-

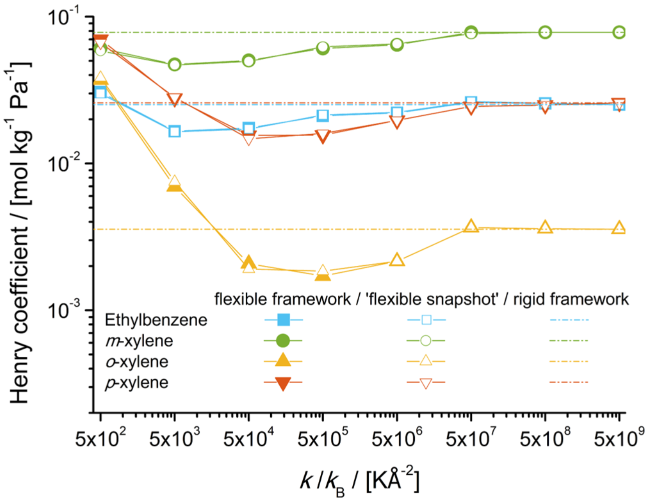

Figure 1. Henry coefficient of ethylbenzene and xylene isomers computed in an MFI-type zeolite at 353 K as a function of framework flexibility k. Closed symbols denote the computations using the flexible framework. Open symbols denote the computations using the "flexible snapshot" method.[90] Dashed lines denote the computations using the rigid framework.

type zeolite. When the framework is very flexible (i.e., k/k_B = 500 KÅ^{-2}), the Henry coefficients of ethylbenzene, p-xylene, and o-xylene are higher than those computed for the structure with atom positions fixed to the crystallographic data (rigid framework). When 5×10^4 KÅ^{-2} $\leq k/k_B \leq 5 \times 10^6$ KÅ^{-2}, the Henry coefficients of ethylbenzene and xylene isomers are lower than that in the rigid zeolite framework.

When $k/k_B > 5 \times 10^7$ KÅ^{-2}, the Henry coefficient of ethylbenzene and xylene isomers is in agreement with the Henry coefficient computed for the rigid structure. This suggests that when k is sufficiently high, framework flexibility does not affect the zeolite structure.

The Henry coefficients of aromatics in MFI-type zeolites computed with the "flexible snapshot" method are in excellent agreement with the values computed using the flexible framework for all k. This suggests that the snapshots can be used to describe the changes that framework flexibility induces on the empty zeolite structure. The mean displacement of the zeolite atoms compared to the rigid structure,[97] the HVF, and the PSD is computed for the five snapshots used in the "flexible snapshot" method. Figure 2 shows the mean displacement of the zeolite framework atoms compared to the rigid framework, the HVF, and the PSD, as a function of k, computed for five MFI-type zeolite snapshots. It is observed that as k is decreased, the mean displacement of the framework atoms increases. When $k/k_B = 5 \times 10^2$ KÅ^{-2}, an average displacement of 0.95 Å is observed. For $k/k_B > 5 \times 10^7$ KÅ^{-2}, the average displacement of framework atoms is close to zero. The HVF of the MFI-type zeolite structures is significantly influenced by framework flexibility. The highest HVF is observed when $k/k_B = 5 \times 10^2$ KÅ^{-2}. For 5×10^4 KÅ^{-2} $\leq k/k_B \leq 5 \times 10^5$ KÅ^{-2}, the HVF of the MFI-type zeolite structure is lower than the HVF computed for the rigid framework. For $k/k_B > 5 \times 10^6$ KÅ^{-2}, the HVF of the MFI-type zeolite structures is in good agreement with the HVF computed for the rigid zeolite structure. The influence of framework flexibility on the HVF shows that the accessible pore volume of the zeolite is directly related to the Henry coefficient of aromatics in MFI-type zeolites.

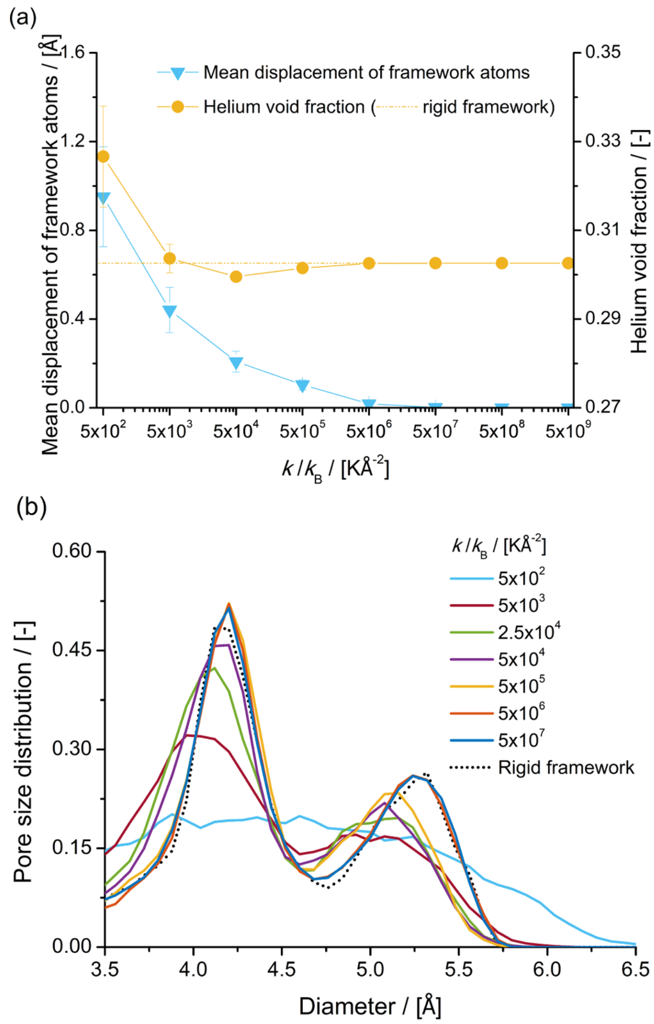

Figure 2. (a) Mean displacement of framework atoms compared to the rigid structure[97] and HVF and (b) PSD of the five empty MFI-type zeolite snapshots used for the "flexible snapshot" method[90] at 353 K as a function of framework flexibility k.

For the PSD of MFI-type zeolites, the peak centered at a diameter of approximately 4.3 Å corresponds to the zigzag and straight channels. The peak centered at a diameter of approximately 5.5 Å corresponds to the intersection of the channels. The PSD of the MFI-type zeolite snapshots shows the influence of framework flexibility on the zeolite pore sizes. It can be observed that as k is decreased, the peak that corresponds to the intersections is shifted to lower diameters. The peak that corresponds to the channels is shifted to lower diameters when $k/k_B \leq 5 \times 10^4$ KÅ^{-2}.

The PSD of the MFI-type structures when $k/k_B = 5 \times 10^2$ KÅ^{-2} does not show a pore size peak distinction between channels and intersection. The maximum pore size observed is 6.5 Å, suggesting that for very high framework flexibility, the deformation of the zeolite void spaces is very large.

As framework flexibility changes the pore size of the zeolite intersections and channels, a decrease of the pore size of the intersection directly affects the adsorption of molecules, and Henry coefficients lower than that for the rigid framework are obtained. This suggests that the interaction of the aromatic molecules and the zeolite framework is highly influenced by changes on the pore sizes of the zeolite. Higher Henry coefficients of aromatic molecules than that in the rigid

https://dx.doi.org/10.1021/acs.jpcc.0c08054
J. Phys. Chem. C 2020, 124, 24488−24499

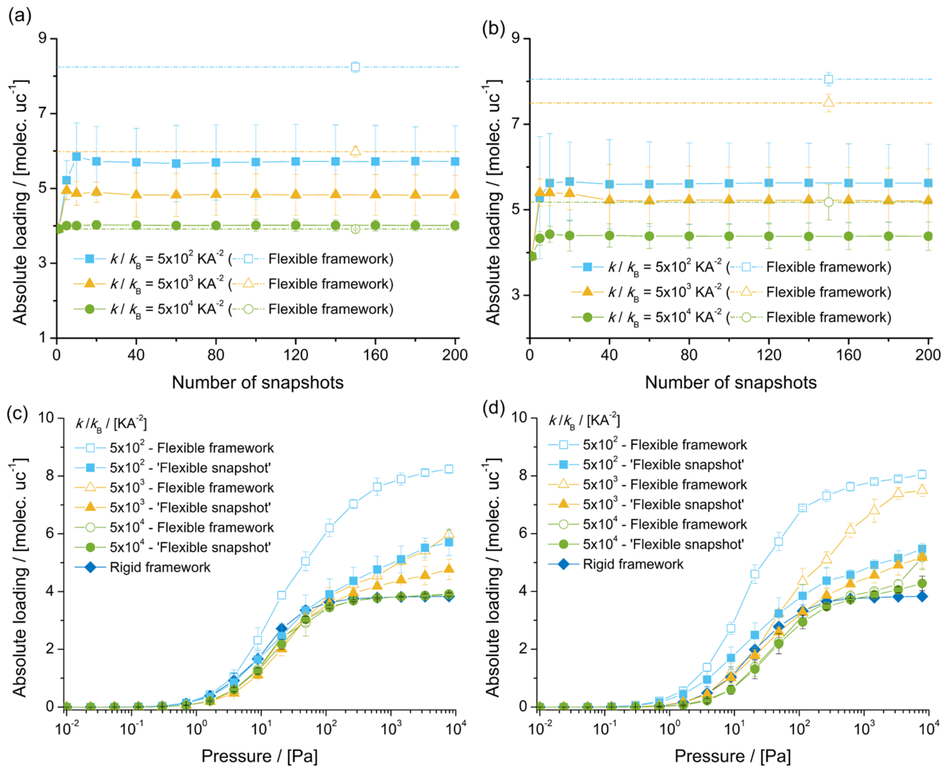

Figure 3. Absolute loadings of (a) ethylbenzene and (b) *p*-xylene at 7848 Pa in an MFI-type zeolite[97] at 353 K computed using the flexible framework and the "flexible snapshot" method, as a function of the number of snapshots considered in the "flexible snapshot" method, for different framework flexibility *k*. Adsorption isotherms of (c) ethylbenzene and (d) *p*-xylene in an MFI-type zeolite[97] at 353 K computed using the flexible framework and the "flexible snapshot" method using ten snapshots for different framework flexibility *k*.

framework when $k/k_B \leq 5 \times 10^3$ KÅ^{-2} can be related to an increase in the size of pores with a diameter of approximately 4.7 Å. The PSDs suggest that as *k* is decreased, the pore sizes of the channels and the intersections become uniform. When $k/k_B = 5 \times 10^6$ KÅ^{-2}, a mean displacement of 0.018 Å of the zeolite atoms is enough to induce up to a 42% decrease of the Henry coefficient of *o*-xylene in MFI-type zeolites compared to the Henry coefficient computed in the rigid framework. With framework flexibility in the range of the original Demontis model (i.e., $k/k_B = 5 \times 10^4$ KÅ^{-2}), Henry coefficients lower than that in the rigid framework are obtained. As the framework is more flexible, Henry coefficients higher than that in the rigid framework are obtained. This suggests that the interactions between the aromatic molecules and the zeolite framework are very susceptible to small displacements of the zeolite atoms and the geometry of the zeolite pores.

Knowledge regarding the effect of loading in the pores of the zeolite as a function of framework flexibility would be of interest. However, a characterization of a flexible framework as a function of loading is cumbersome. A given loading may have several adsorbate configurations in the framework. Sampling the effect of all these configurations in the framework for a given loading is computationally expensive. Therefore, the effect of framework flexibility on the zeolite framework was only estimated for an empty zeolite framework.

Since the snapshots are obtained from an empty zeolite structure, the capacity of the "flexible snapshot" method to describe the adsorption of aromatics outside the Henry regime is of interest. Simulations of adsorption of ethylbenzene and *p*-xylene in an MFI-type structure are computed at 7848 Pa, using different number of snapshots, for different *k*. Snapshot 1 corresponds to the crystal structure from experiments.[97] The loadings of ethylbenzene and *p*-xylene in MFI-type zeolite at 7848 Pa and 353 K as a function of the number of snapshots for different *k* are shown in Figure 3. The loadings computed using the "flexible snapshot" method are higher than the loadings computed in the rigid framework. The loadings computed with the "flexible snapshot" method are lower than the loadings obtained using a flexible framework. It can be observed that the loadings using the "flexible snapshot" method do not depend on the number of snapshots used if ten or more snapshots are used. Adsorption isotherms of ethylbenzene and *p*-xylene in an MFI-type zeolite at 353 K are computed using the flexible framework and the "flexible snapshot" method with ten snapshots are shown in Figure 3. The adsorption isotherms show the differences between the loadings computed with the flexible framework and the "flexible snapshot" method. In the "flexible snapshot" method, it is assumed that the adsorbate does not have a significant effect on the framework dynamics.[92] This assumption has a significant effect on the computed loadings when framework flexibility is high (i.e., *k* is low). When $k/k_B = 5 \times 10^2$ KÅ^{-2}, significant differences between the loadings of ethylbenzene and *p*-xylene in MFI-type zeolite computed with the flexible framework and the "flexible snapshot" method are observed for pressures higher than 10 Pa. For framework flexibility $k/k_B = 5 \times 10^3$ KÅ^{-2} and $k/k_B = 5 \times 10^4$ KÅ^{-2}, the loading differences can be observed when the pressure is higher than 100 Pa, and loadings higher than 4 molec./u.c. are obtained. The "flexible snapshot" method can be used to understand the effect that bulky aromatic guest molecules produce on the zeolite framework. It can be observed that the loadings computed

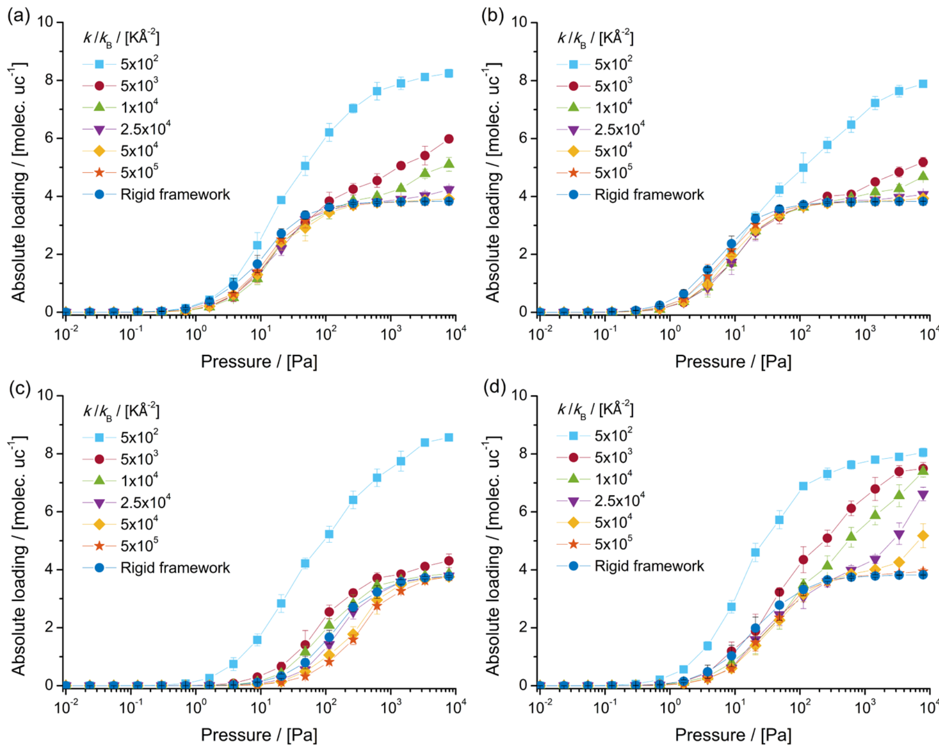

Figure 4. Adsorption isotherms for (a) ethylbenzene, (b) *m*-xylene, (c) *o*-xylene, and (d) *p*-xylene in an MFI-type zeolite[97] at 353 K, varying framework flexibility *k*.

using the "flexible snapshot" method account for the molecules that would fit in a new rigid framework with the new average configuration produced by a particular framework flexibility *k*. The difference between the loadings computed with the "flexible snapshot" method and the flexible framework correspond to the effect on the isotherm of how the framework accommodates to the guest molecules. The "flexible snapshot" method is useful for the description of the adsorption behavior at very low loadings/infinite dilution. For high pressures/loadings, the "flexible snapshot" method does not yield the same loading as when the flexible framework is used. This suggests that the effect of the guest aromatic molecules on the zeolite framework should not be neglected.

Adsorption isotherms of ethylbenzene and xylene isomers at 353 K in an MFI-type zeolite varying framework flexibility *k* are shown in Figure 4. Framework flexibility influences the adsorption isotherm of aromatics in MFI-type zeolite. In the low pressure regime (i.e., $P < 10^2$ Pa), the loadings of ethylbenzene are similar for $k/k_B \geq 5 \times 10^3$ KÅ^{-2}. At higher pressures, the effect of framework flexibility is observed, yielding higher loadings as *k* is decreased. The highest loadings of ethylbenzene in the considered pressure range are obtained when $k/k_B = 5 \times 10^2$ KÅ^{-2}, having up to 8.2 molec./u.c. at 7848 Pa.

At pressures lower than 20 Pa, framework flexibility does not play a role in the loadings of *m*-xylene. When $k/k_B = 5 \times 10^2$ KÅ^{-2}, loadings of 7.8 molec./u.c. of *m*-xylene are observed at 7848 Pa. For 5×10^3 KÅ^{-2} $\leq k/k_B \leq 10^4$ KÅ^{-2}, framework flexibility influences adsorption only when the pressure is higher than 6×10^2 Pa. Figure 5 shows two typical snapshots of the simulation of adsorption of *m*-xylene in an MFI-type zeolite at 353 K and 7848 Pa, using a rigid zeolite framework (Figure 5a) and a flexible zeolite framework with $k/k_B = 5 \times 10^2$ KÅ^{-2} (Figure 5b). It can be observed that when using the rigid zeolite framework, *m*-xylene molecules are located exclusively in the intersection of the zigzag and the straight channel. When $k/k_B = 5 \times 10^2$ KÅ^{-2}, *m*-xylene molecules are located in the intersections of the channels, as well as in the channels.

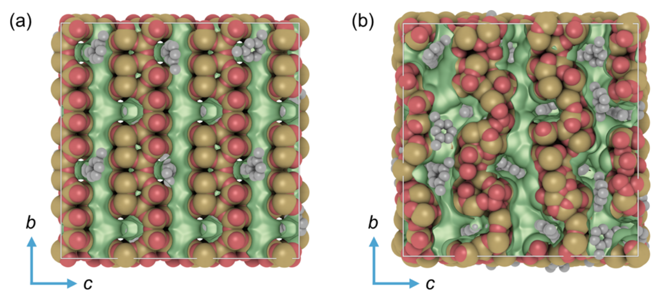

Figure 5. Typical snapshots of the simulations of adsorption of *m*-xylene in an MFI-type zeolite at 353 K and 7848 Pa. (a) Simulation using the rigid zeolite framework. (b) Simulations using framework flexibility $k/k_B = 5 \times 10^2$ KÅ^{-2}. The green area denotes the adsorption surface computed with iRASPA.[107]

Unlike ethylbenzene and *m*-xylene, *o*-xylene adsorption is affected by framework flexibility already at very low pressures. The effects of framework flexibility are noticeable when the pressure is higher than 10 Pa. Framework flexibility has a significant influence on the Henry coefficient of *o*-xylene (Figure 1); the Henry coefficient of *o*-xylene is 1.9 times higher than that for the rigid structure when $k/k_B = 5 \times 10^3$ KÅ^{-2} and 0.48 times smaller than that for the rigid structure when $k/k_B = 5 \times 10^5$ KÅ^{-2}. This suggests that the adsorption of *o*-xylene in MFI-type zeolite is sensitive to the changes of the zeolite structure caused by framework flexibility already at low loadings. When $k/k_B = 5 \times 10^2$ KÅ^{-2}, *o*-xylene loadings of up to 8.5 molec./u.c. are obtained. For $k/k_B = 5 \times 10^3$ KÅ^{-2},

https://dx.doi.org/10.1021/acs.jpcc.0c08054
J. Phys. Chem. C 2020, 124, 24488−24499

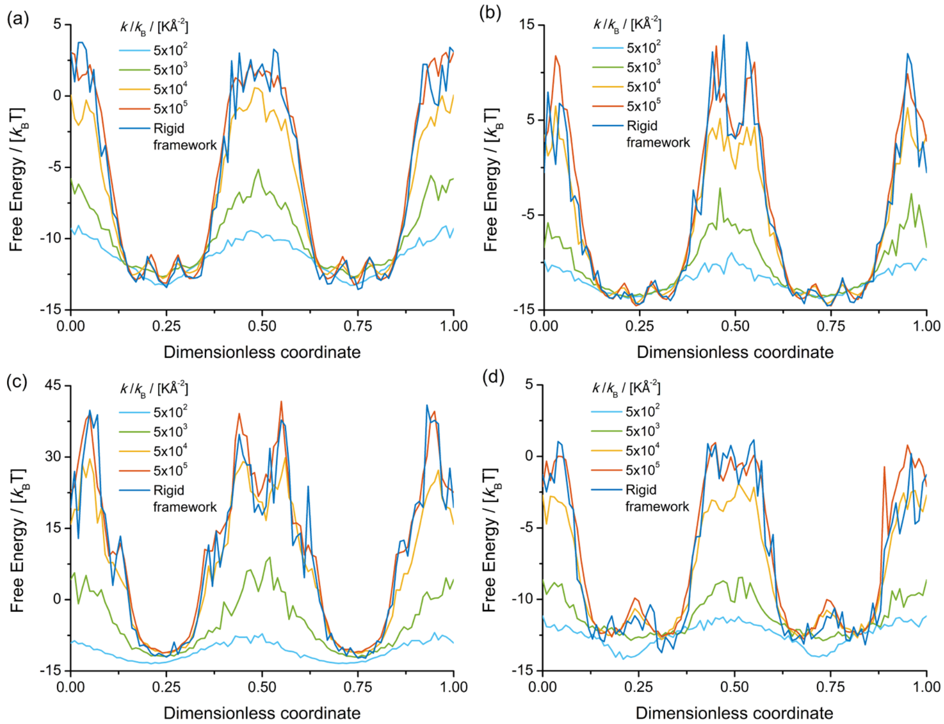

Figure 6. Free-energy profiles in the *b*-crystallographic axis (parallel to the straight channel) for (a) ethylbenzene, (b) *m*-xylene, (c) *o*-xylene, and (d) *p*-xylene at infinite dilution in an MFI-type zeolite[97] at 353 K, varying framework flexibility *k*. The dimensionless coordinate correspond to the dimensionless position across the *b*-crystallographic axis of the MFI-type zeolite unit cell.

the maximum loading obtained is 4.3 molec./u.c. As $k/k_B \geq 10^4$ KÅ^{-2}, maximum loadings of approximately 3.8 molec./u.c. are obtained. *p*-Xylene adsorption is highly affected by framework flexibility, especially at high pressures. The maximum loading of *p*-xylene (8.1 molec./u.c.) is obtained for $k/k_B = 5 \times 10^2$ KÅ^{-2}. Only when $k/k_B \geq 5 \times 10^5$ KÅ^{-2}, the loadings obtained with the flexible framework are the same as the loadings obtained in the rigid framework. In the case of C_8 aromatics, inflection point in the isotherm can be an indication of the occupancy of new adsorption sites,[38] such as the zigzag and straight channels. For adsorption of aromatics in MFI-type zeolites, when the loadings are lower than 4 molec./u.c., the molecules occupy the intersection of the channels. At higher loadings, the molecules occupy the void spaces in the channels. It can be observed that as k is decreased to $k/k_B = 5 \times 10^2$ KÅ^{-2}, the shape of the isotherms for ethylbenzene and xylene isomers changes from type IV to type I. The PSD of the empty zeolite structure for $k/k_B = 5 \times 10^2$ KÅ^{-2} (Figure 2b) shows the absence of a pore size peak distinction between the channels and the intersections. This suggests that the changes that framework flexibility induces in the zeolite structure can change the shape of the adsorption isotherm of aromatics in MFI-type zeolites. To determine optimal values of framework flexibility k, comparison with appropriate experimental data for all the sorbates considered is needed. However, experimental data of adsorption of aromatics in MFI-type zeolites is scarce and not always consistent under the same temperature/pressure conditions.[37] Therefore, the optimal framework flexibility k was not determined in this work.

The free-energy profiles of ethylbenzene and xylene isomers in an MFI-type zeolite as a function of framework flexibility are shown in Figure 6. The dimensionless coordinate correspond to the dimensionless position across the *b*-crystallographic axis of the MFI-type zeolite unit cell. The free-energy profiles suggest that framework flexibility significantly influences the free-energy barrier between the low energy states (intersections). As k is decreased, the free-energy barrier between the intersections of the channels is decreased. This suggests that the pore size changes that framework flexibility induces on the zeolite framework have an important effect on the free-energy of aromatic molecules in MFI-type zeolites.

The free-energy profiles are used to compute the hopping rate $k^{TST}_{A\to B}$ and the self-diffusion coefficient (D) at infinite dilution of aromatics in the straight channel of an MFI-type zeolite framework using TST. Estimations of the self-diffusion coefficients of aromatics at high loadings or for the zigzag channel of MFI-type zeolite are not computed in this work. In TST, it is assumed that all particles that reach the free-energy barrier from a low energy site A to a low energy site B eventually end up in B.[80] In reality, not all the molecules at the dividing surface actually diffuse through the pores.[83] A dynamical correction can be computed to account for this factor.[83,84] To study the effect of framework flexibility on the diffusion of aromatics in MFI-type zeolites, only an estimation of the diffusion coefficient is used. The dynamical correction was not included in this work as it is computationally expensive to determine. The hopping rates $k^{TST}_{A\to B}$ are obtained by computing the relative probability to find a molecule on top of the free-energy barrier, and the velocity of the molecule is given by a Maxwell distribution corresponding to the temperature of the system.[17] The hopping distance $\lambda_{A\to B}$ is the distance between A and B. At infinite dilution, the self-diffusion coefficient is calculated using the expression $D = k^{TST}_{A\to B} \cdot \lambda_{A\to B}{}^2$. The reader is referred to refs[17,80,83,84] for details about the calculation of diffusion coefficients from TST. The self-diffusion coefficients of ethylbenzene and xylene isomers in the straight channel of MFI-type zeolite at 353 K are shown in Figure 7. It can be observed that framework flexibility has an

https://dx.doi.org/10.1021/acs.jpcc.0c08054
J. Phys. Chem. C 2020, 124, 24488−24499

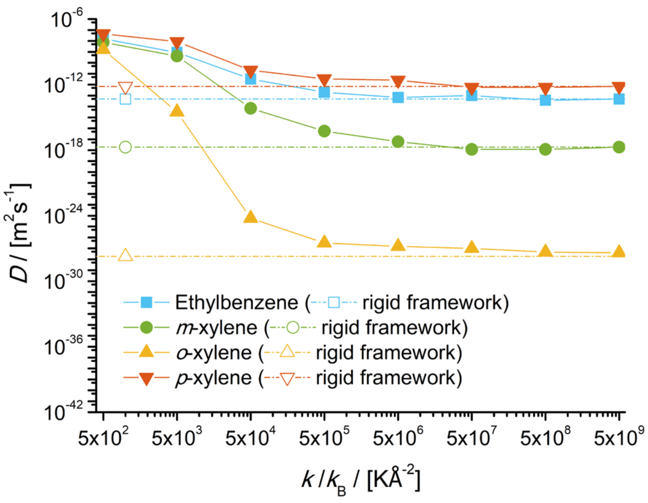

Figure 7. Self-diffusion coefficient D computed using TST for ethylbenzene and xylene isomers in the straight channel of an MFI-type zeolite[97] at 353 K, varying framework flexibility k.

important effect on the self-diffusion coefficient of aromatics in MFI-type zeolites. The highest self-diffusivity coefficients D are obtained when $k/k_B = 5 \times 10^2$ $KÅ^{-2}$ for all aromatics considered. As k is increased, the computed D is in agreement with the self-diffusion coefficient computed in the rigid framework. For all values of k considered (and the rigid structures), $D_{p\text{-xylene}} > D_{\text{ethylbenzene}} > D_{m\text{-xylene}} > D_{o\text{-xylene}}$. Comparing the self-diffusion coefficients obtained when $k/k_B = 5 \times 10^2$ $KÅ^{-2}$ and D obtained in the rigid structure, framework flexibility affects the diffusion of aromatic molecules in an MFI-type zeolite differently: $D_{\text{ethylbenzene}}$ increased from 4.7×10^{-14} to 1.5×10^{-8} m^2 s^{-1}; $D_{m\text{-xylene}}$ increased from 1.9×10^{-18} to 7.6×10^{-9} m^2 s^{-1}; $D_{o\text{-xylene}}$ increased from 1.9×10^{-28} to 1.6×10^{-9} m^2 s^{-1}; and $D_{p\text{-xylene}}$ increased from 6.8×10^{-13} to 4.5×10^{-8} m^2 s^{-1}. Framework flexibility significantly changes D when $k/k_B \leq 5 \times 10^6$ $KÅ^{-2}$. This suggests that the changes that framework flexibility induces on the pore sizes of the channels of the zeolite framework notably influence the estimation of D.

4. CONCLUSIONS

The influence of framework flexibility on the adsorption and diffusion behavior of C_8 aromatics in an MFI-type zeolite has been investigated using molecular simulations. It has been observed that—regardless of taking the bond lengths and angles from the crystallographic data—framework flexibility induces changes on the average zeolite structure. As the framework is more flexible, it is difficult to discriminate the channels and the intersections based on pore sizes. This has a significant effect on the Henry coefficient and the adsorption isotherms of aromatics in MFI-type zeolites. The Henry coefficient of aromatics in MFI-type zeolites is significantly affected by framework flexibility. With framework flexibility in the range of the original Demontis model (i.e., $k/k_B = 5 \times 10^4$ $KÅ^{-2}$), computed Henry coefficients of aromatics in MFI-type zeolites are lower than that in the rigid framework. As the framework is more flexible, Henry coefficients are higher than that in the rigid framework. When $k/k_B = 5 \times 10^6$ $KÅ^{-2}$, a mean displacement of the zeolite atoms of 0.018 Å is enough to induce a significant change in the Henry coefficient of aromatics in MFI-type zeolites. This suggests that the interactions between the aromatic molecules and the zeolite framework are very susceptible to small displacements of the zeolite atoms and changes of the geometry of the zeolite pores. The "flexible snapshot" method is useful for the description of the adsorption behavior at very low loadings/infinite dilution. For high pressures/loadings, the "flexible snapshot" method does not yield the same loading as when the flexible framework is used. This suggests that the effect of the guest molecules on the zeolite framework should not be neglected. For using the "flexible snapshot" method at high loadings, a loaded framework could be considered to create snapshots that yield estimation of the loadings closer to simulations using a fully flexible framework. However, the computational cost of creating such snapshots with energy equilibrated adsorbates is equivalent to the simulation of a loaded fully flexible framework, and hence the "flexible snapshot" method is not considered further. The adsorption isotherms are affected by framework flexibility. At low loadings, the influence of the framework flexibility on the adsorption is small. When the loadings are higher than 4 molec./u.c., lower framework flexibility k yields higher loadings than that in the rigid framework. For the pressure range considered, the maximum loadings of aromatics in MFI-type zeolites computed depend on the framework flexibility. Higher maximum loadings are obtained when the framework is more flexible (i.e., $k/k_B = 5 \times 10^2$ $KÅ^{-2}$). For ethylbenzene, m-xylene, and p-xylene, framework flexibility plays an important role when the loadings are higher than 4 molec./u.c. For o-xylene, framework flexibility plays a role when the loadings are lower than 4 molec./u.c. The changes that framework flexibility induces in the zeolite structure can change the shape of the adsorption isotherm of aromatics in MFI-type zeolites for very flexible zeolite frameworks. Framework flexibility significantly decreases the free-energy barriers of aromatics between the low energy sites of the zeolite framework. As the zeolite framework is more flexible, the self-diffusion coefficient is significantly increased. Framework flexibility has a remarkable effect on the adsorption and diffusion of aromatics in MFI-type zeolites. The simulations from this work suggest that framework flexibility is important for systems with molecules fitting tightly in nonporous materials. Similar effects of framework flexibility may be found for other classes of porous materials, and studies addressing this topic are encouraged. However, materials such as MOFs can have large-scale structural rearrangements that may need different approaches. In the future, the development of force fields for zeolite framework flexibility should have a special focus on the interactions of bulky aromatic guest molecules with and within a zeolite framework.

AUTHOR INFORMATION

Corresponding Author

Thijs J. H. Vlugt − *Engineering Thermodynamics, Process & Energy Department, Faculty of Mechanical, Maritime and Materials Engineering, Delft University of Technology, 2628 CB Delft, The Netherlands*; Email: t.j.h.vlugt@tudelft.nl

Authors

Sebastián Caro-Ortiz − *Engineering Thermodynamics, Process & Energy Department, Faculty of Mechanical, Maritime and Materials Engineering, Delft University of Technology, 2628 CB Delft, The Netherlands*

Erik Zuidema − *Shell Global Solutions International B.V., 1030 BN Amsterdam, The Netherlands*

https://dx.doi.org/10.1021/acs.jpcc.0c08054
J. Phys. Chem. C 2020, 124, 24488−24499

Marcello Rigutto − *Shell Global Solutions International B.V., 1030 BN Amsterdam, The Netherlands*
David Dubbeldam − *Van 't Hoff Institute of Molecular Sciences, University of Amsterdam, 1098 XH Amsterdam, The Netherlands;* orcid.org/0000-0002-4382-1509

Complete contact information is available at: https://pubs.acs.org/10.1021/acs.jpcc.0c08054

Notes

The authors declare no competing financial interest.

■ ACKNOWLEDGMENTS

The authors gratefully acknowledge financial support from Shell Global Solutions International B.V. This work was sponsored by NWO Exacte Wetenschappen (Physical Sciences) for the use of supercomputer facilities with financial support from the Nederlandse Organisatie voor Wetenschappelijk Onderzoek (Netherlands Organization for Scientific Research, NWO). T.J.H.V. acknowledges NWO-CW for a VICI grant.

■ REFERENCES

(1) Primo, A.; Garcia, H. Zeolites as catalysts in oil refining. *Chem. Soc. Rev.* **2014**, *43*, 7548−7561.
(2) Karge, H. G.; Weitkamp, J. *Zeolites as Catalysts, Sorbents and Detergent Builders: Applications and Innovations*; Elsevier, 1989.
(3) Cai, L.; Koziel, J. A.; Liang, Y.; Nguyen, A. T.; Xin, H. Evaluation of zeolite for control of odorants emissions from simulated poultry manure storage. *J. Environ. Qual.* **2007**, *36*, 184−193.
(4) Valdés, H.; Alejandro, S.; Zaror, C. A. Natural zeolite reactivity towards ozone: The role of compensating cations. *J. Hazard. Mater.* **2012**, *227*−*228*, 34−40.
(5) Van Speybroeck, V.; Hemelsoet, K.; Joos, L.; Waroquier, M.; Bell, R. G.; Catlow, C. R. A. Advances in theory and their application within the field of zeolite chemistry. *Chem. Soc. Rev.* **2015**, *44*, 7044−7111.
(6) Kubuå, M.; Millini, R.; Zilkova, N. 10-ring Zeolites: Synthesis, characterization and catalytic applications. *Catal. Today* **2019**, *324*, 3−14.
(7) Ozaydin, S.; Kocer, G.; Hepbasli, A. Natural zeolites in energy applications. *Energy Sources, Part A* **2006**, *28*, 1425−1431.
(8) Luna-Triguero, A.; Vicent-Luna, J. M.; Jansman, M. J.; Zafeiropoulos, G.; Tsampas, M. N.; van de Sanden, M. C. M.; Akse, H. N.; Calero, S. Enhancing separation efficiency in European syngas industry by using zeolites. *Catal. Today* **2020**, DOI: 10.1016/j.cattod.2020.03.061. , in press
(9) Sweeney, W. A.; Bryan, P. F. BTX Processing. *Kirk*−*Othmer Encyclopedia of Chemical Technology*; American Cancer Society, 2000.
(10) Bellussi, G. In *Recent Advances in the Science and Technology of Zeolites and Related Materials*; van Steen, E., Claeys, I., Callanan, L., Eds.; Studies in Surface Science and Catalysis; Elsevier, 2004; Vol. *154*; pp 53−65.
(11) Ali, S. A.; Aitani, A. M.; Čejka, J.; Al-Khattaf, S. S. Selective production of xylenes from alkyl-aromatics and heavy reformates over dual-zeolite catalyst. *Catal. Today* **2015**, *243*, 118−127.
(12) Gołąbek, K.; Tarach, K. A.; Góra-Marek, K. Xylenes transformation over zeolites ZSM-5 ruled by acidic properties. *Spectrochim. Acta, Part A* **2018**, *192*, 361−367.
(13) Mihályi, R. M.; Klébert, S.; Kollár, M.; Mavrodinova, V. Transformation of ethylbenzene-m-xylene mixture on zeolites with different structures. *J. Porous Mater.* **2014**, *21*, 485−493.
(14) Toda, J.; Corma, A.; Abudawoud, R. H.; Elanany, M. S.; Al-Zahrani, I. M.; Sastre, G. Influence of force fields on the selective diffusion of para-xylene over ortho-xylene in 10-ring zeolites. *Mol. Simul.* **2015**, *41*, 1438−1448.
(15) Smit, B.; Daniël J C Loyens, L.; Verbist, G. L. M. M. Simulation of adsorption and diffusion of hydrocarbons in zeolites. *Faraday Discuss.* **1997**, *106*, 93−104.
(16) *Zeolites in Industrial Separation and Catalysis*, 1st ed.; Kulprathipanja, S., Ed.; John Wiley & Sons, Ltd., 2010.
(17) Smit, B.; Maesen, T. L. M. Molecular simulations of zeolites: Adsorption, diffusion, and shape selectivity. *Chem. Rev.* **2008**, *108*, 4125−4184.
(18) Vlugt, T. J. H.; Zhu, W.; Kapteijn, F.; Moulijn, J. A.; Smit, B.; Krishna, R. Adsorption of linear and branched alkanes in the zeolite silicalite-1. *J. Am. Chem. Soc.* **1998**, *120*, 5599−5600.
(19) Talu, O.; Guo, C. J.; Hayhurst, D. T. Heterogeneous adsorption equilibria with comparable molecule and pore sizes. *J. Phys. Chem.* **1989**, *93*, 7294−7298.
(20) Lee, C.-K.; Chiang, A. S. T. Adsorption of aromatic compounds in large MFI zeolite crystals. *J. Chem. Soc., Faraday Trans.* **1996**, *92*, 3445−3451.
(21) Sacerdote, M.; Bosselet, F.; Mentzen, B. F. The MFI(ZSM-5)/sorbate systems. Comparison between structural, theoretical and calorimetric results. Part II - The MFI/benzene system. *Mater. Res. Bull.* **1990**, *25*, 593−599.
(22) Fyfe, C. A.; Lee, J. S. J. Solid-state NMR determination of the zeolite ZSM-5/ortho-xylene host-guest crystal structure. *J. Phys. Chem. C* **2008**, *112*, 500−513.
(23) Mentzen, B. F.; Lefebvre, F. Flexibility of the MFI silicalite framework upon benzene adsorption at higher pore-fillings: A study by X-ray power diffraction, NMR and molecular mechanics. *Mater. Res. Bull.* **1997**, *32*, 813−820.
(24) Schumacher, R.; Karge, H. G. Sorption and sorption kinetics of ethylbenzene in MFI-Type zeolites studied by a barometric technique. *Collect. Czech. Chem. Commun.* **1999**, *64*, 483−494.
(25) Wu, P.; Debebe, A.; Ma, Y. H. Adsorption and diffusion of C_6 and C_8 hydrocarbons in silicalite. *Zeolites* **1983**, *3*, 118−122.
(26) Cartarius, R.; Vogel, H.; Dembowski, J. Investigation of sorption and intracrystalline diffusion of benzene and toluene on silicalite-1. *Ber. Bunsen-Ges.* **1997**, *101*, 193−199.
(27) Hill, S. G.; Seddon, D. Comparison of the sorption of benzene in ZSM-5, silicalite-1, and silicalite-2. *Zeolites* **1991**, *11*, 699−704.
(28) Malović, D.; Vučelić, D. Application of thermal analysis for explaining the sorption of benzene and n-hexane on silicalite. *J. Therm. Anal. Calorim.* **1998**, *53*, 835−842.
(29) Song, L.; Sun, Z.; Duan, L.; Gui, J.; McDougall, G. S. Adsorption and diffusion properties of hydrocarbons in zeolites. *Microporous Mesoporous Mater.* **2007**, *104*, 115−128.
(30) Richards, R. E.; Rees, L. V. C. The sorption of p-xylene in ZSM-5. *Zeolites* **1988**, *8*, 35−39.
(31) Ban, H.; Gui, J.; Duan, L.; Zhang, X.; Song, L.; Sun, Z. Sorption of hydrocarbons in silicalite-1 studied by intelligent gravimetry. *Fluid Phase Equilib.* **2005**, *232*, 149−158.
(32) Thamm, H. Calorimetric study on the state of aromatic molecules sorbed on silicalite. *J. Phys. Chem.* **1987**, *91*, 8−11.
(33) Rudziński, W.; Narkiewicz-Michałek, J.; Szabelski, P.; Chiang, A. S. T. Adsorption of aromatics in zeolites ZSM-5: A thermodynamic-calorimetric study based on the model of adsorption on heterogeneous adsorption sites. *Langmuir* **1997**, *13*, 1095−1103.
(34) Rodeghero, E.; Chenet, T.; Martucci, A.; Ardit, M.; Sarti, E.; Pasti, L. Selective adsorption of toluene and n-hexane binary mixture from aqueous solution on zeolite ZSM-5: Evaluation of competitive behavior between aliphatic and aromatic compounds. *Catal. Today* **2019**, *345*, 157−164.
(35) Nair, S.; Tsapatsis, M. The location of o- and m-xylene in silicalite by powder X-ray diffraction. *J. Phys. Chem. B* **2000**, *104*, 8982−8988.
(36) Gobin, O. C.; Reitmeier, S. J.; Jentys, A.; Lercher, J. A. Diffusion pathways of benzene, toluene and p-xylene in MFI. *Microporous Mesoporous Mater.* **2009**, *125*, 3−10.
(37) Caro-Ortiz, S.; Zuidema, E.; Dekker, D.; Rigutto, M.; Dubbeldam, D.; Vlugt, T. J. H. Adsorption of aromatics in MFI-

type zeolites: experiments and framework flexibility in Monte Carlo simulations. *J. Phys. Chem. C* **2020**, *124*, 21782−21797.

(38) Poursaeidesfahani, A.; Torres-Knoop, A.; Rigutto, M.; Nair, N.; Dubbeldam, D.; Vlugt, T. J. H. Computation of the heat and entropy of adsorption in proximity of inflection points. *J. Phys. Chem. C* **2016**, *120*, 1727−1738.

(39) Smit, B.; Maesen, T. L. M. Commensurate 'freezing' of alkanes in the channels of a zeolite. *Nature* **1995**, *374*, 42−44.

(40) Floquet, N.; Coulomb, J. P.; Weber, G.; Bertrand, O.; Bellat, J. P. Structural signatures of type IV isotherm steps: Sorption of trichloroethene, tetrachloroethene, and benzene in silicalite-I. *J. Phys. Chem. B* **2003**, *107*, 685−693.

(41) Fyfe, C. A.; Strobl, H.; Kokotailo, G. T.; Kennedy, G. J.; Barlow, G. E. Ultrahigh-resolution silicon-29 solid-state MAS NMR investigation of sorbate and temperature-induced changes in the lattice structure of zeolite ZSM-5. *J. Am. Chem. Soc.* **1988**, *110*, 3373−3380.

(42) de Vos Burchart, E.; van Bekkum, H.; van de Graaf, B. Molecular mechanics studies on MFI-type zeolites: Part 3. The monoclinic-orthorhombic phase transition. *Zeolites* **1993**, *13*, 212−215.

(43) Ilić, B.; Wettstein, S. G. A review of adsorbate and temperature-induced zeolite framework flexibility. *Microporous Mesoporous Mater.* **2017**, *239*, 221−234.

(44) Song, L.; Rees, L. V. C. Adsorption and diffusion of cyclic hydrocarbon in MFI-type zeolites studied by gravimetric and frequency-response techniques. *Microporous Mesoporous Mater.* **2000**, *35*−*36*, 301−314.

(45) van Koningsveld, H.; Tuinstra, F.; van Bekkum, H.; Jansen, J. C. The location of p-xylene in a single crystal of zeolite H-ZSM-5 with a new, sorbate-induced, orthorhombic framework symmetry. *Acta Crystallogr., Sect. B: Struct. Sci.* **1989**, *45*, 423−431.

(46) Calero, S. In *Modeling of Transport and Accessibility in Zeolites*; Cejka, J., Corma, A., Zones, S., Eds.; Zeolites and Catalysis; John Wiley & Sons, Ltd., 2010; pp 335−360.

(47) Fang, H.; Demir, H.; Kamakoti, P.; Sholl, D. S. Recent developments in first-principles force fields for molecules in nanoporous materials. *J. Mater. Chem. A* **2014**, *2*, 274−291.

(48) Ungerer, P.; Tavitian, B.; Boutin, A. *Applications of Molecular Simulation in the Oil and Gas Industry—Monte-Carlo Methods*, 1st ed.; Editions Technip, 2005.

(49) Snurr, R. Q.; Bell, A. T.; Theodorou, D. N. Prediction of adsorption of aromatic hydrocarbons in silicalite from grand canonical Monte Carlo simulations with biased insertions. *J. Phys. Chem.* **1993**, *97*, 13742−13752.

(50) Li, J.; Talu, O. Structural effect on molecular simulations of tight-pore systems. *J. Chem. Soc., Faraday Trans.* **1993**, *89*, 1683−1687.

(51) Torres-Knoop, A.; Heinen, J.; Krishna, R.; Dubbeldam, D. Entropic separation of styrene/ethylbenzene mixtures by exploitation of subtle differences in molecular configurations in ordered crystalline nanoporous adsorbents. *Langmuir* **2015**, *31*, 3771−3778.

(52) Mohanty, S.; Davis, H. T.; McCormick, A. V. Shape selective adsorption in atomistic nanopores - a study of xylene isomers in silicalite. *Chem. Eng. Sci.* **2000**, *55*, 2779−2792.

(53) Chempath, S.; Snurr, R. Q.; Low, J. J. Molecular modeling of binary liquid-phase adsorption of aromatics in silicalite. *AIChE J.* **2004**, *50*, 463−469.

(54) Sánchez-Gil, V.; Noya, E. G.; Sanz, A.; Khatib, S. J.; Guil, J. M.; Lomba, E.; Marguta, R.; Valencia, S. Experimental and simulation studies of the stepped adsorption of toluene on pure-silica MEL zeolite. *J. Phys. Chem. C* **2016**, *120*, 8640−8652.

(55) Zeng, Y.; Moghadam, P. Z.; Snurr, R. Q. Pore size dependence of adsorption and separation of thiophene/benzene mixtures in zeolites. *J. Phys. Chem. C* **2015**, *119*, 15263−15273.

(56) Yue, X.; Yang, X. Molecular simulation study of adsorption and diffusion on silicalite for a benzene/CO_2 mixture. *Langmuir* **2006**, *22*, 3138−3147.

(57) Zeng, Y.; Ju, S.; Xing, W.; Chen, C. Computer simulation of the adsorption of thiophene/benzene mixtures on MFI and MOR. *Sep. Purif. Technol.* **2007**, *55*, 82−90.

(58) Ban, S.; van Laak, A.; de Jongh, P. E.; van der Eerden, J. P. J. M.; Vlugt, T. J. H. Adsorption selectivity of benzene/propene mixtures for various zeolites. *J. Phys. Chem. C* **2007**, *111*, 17241−17248.

(59) Cosoli, P.; Fermeglia, M.; Ferrone, M. GCMC simulations in zeolite MFI and activated carbon for benzene removal from exhaust gaseous streams. *Mol. Simul.* **2008**, *34*, 1321−1327.

(60) Jeffroy, M.; Fuchs, A. H.; Boutin, A. Structural changes in nanoporous solids due to fluid adsorption: thermodynamic analysis and Monte Carlo simulations. *Chem. Commun.* **2008**, 3275−3277.

(61) Krishna, R.; van Baten, J. M. Influence of adsorption thermodynamics on guest diffusivities in nanoporous crystalline materials. *Phys. Chem. Chem. Phys.* **2013**, *15*, 7994−8016.

(62) Boulet, P.; Narasimhan, L.; Berg'e-Lefranc, D.; Kuchta, B.; Schäf, O.; Denoyel, R. Adsorption into the MFI zeolite of aromatic molecule of biological relevance. Investigations by Monte Carlo simulations. *J. Mol. Model.* **2009**, *15*, 573−579.

(63) Jeffroy, M.; Nieto-Draghi, C.; Boutin, A. Molecular simulation of zeolite flexibility. *Mol. Simul.* **2014**, *40*, 6−15.

(64) Sartbaeva, A.; Wells, S. A.; Treacy, M. M. J.; Thorpe, M. F. The flexibility window in zeolites. *Nat. Mater.* **2006**, *5*, 962−965.

(65) Vlugt, T. J. H.; Schenk, M. Influence of framework flexibility on the adsorption properties of hydrocarbons in the zeolite silicalite. *J. Phys. Chem. B* **2002**, *106*, 12757−12763.

(66) Fuchs, A. H.; Cheetham, A. K. Adsorption of guest molecules in zeolitic materials: Computational aspects. *J. Phys. Chem. B* **2001**, *105*, 7375−7383.

(67) Clark, L. A.; Snurr, R. Q. Adsorption isotherm sensitivity to small changes in zeolite structure. *Chem. Phys. Lett.* **1999**, *308*, 155−159.

(68) Schenk, M.; Smit, B.; Maesen, T. L. M.; Vlugt, T. J. H. Molecular simulations of the adsorption of cycloalkanes in MFI-type silica. *Phys. Chem. Chem. Phys.* **2005**, *7*, 2622−2628.

(69) Dubbeldam, D.; Walton, K. S.; Vlugt, T. J. H.; Calero, S. Design, parameterization, and implementation of atomic force fields for adsorption in nanoporous materials. *Adv. Theory Simul.* **2019**, *2*, 1900135.

(70) Park, J.; Agrawal, M.; Sava Gallis, D. F.; Harvey, J. A.; Greathouse, J. A.; Sholl, D. S. Impact of intrinsic framework flexibility for selective adsorption of sarin in non-aqueous solvents using metal−organic frameworks. *Phys. Chem. Chem. Phys.* **2020**, *22*, 6441−6448.

(71) Kupgan, G.; Demidov, A. G.; Colina, C. M. Plasticization behavior in polymers of intrinsic microporosity (PIM-1): A simulation study from combined Monte Carlo and Molecular Dynamics. *J. Membr. Sci.* **2018**, *565*, 95−103.

(72) Rogge, S. M. J.; Goeminne, R.; Demuynck, R.; Gutiérrez-Sevillano, J. J.; Vandenbrande, S.; Vanduyfhuys, L.; Waroquier, M.; Verstraelen, T.; Van Speybroeck, V. Modeling gas adsorption in flexible Metal−Organic Frameworks via Hybrid Monte Carlo/Molecular Dynamics schemes. *Adv. Theory Simul.* **2019**, *2*, 1800177.

(73) Chokbunpiam, T.; Fritzsche, S.; Caro, J.; Chmelik, C.; Janke, W.; Hannongbua, S. Importance of ZIF-90 lattice flexibility on diffusion, permeation, and lattice structure for an adsorbed H2/CH4 gas mixture: A re-examination by Gibbs ensemble Monte Carlo and Molecular Dynamics simulations. *J. Phys. Chem. C* **2017**, *121*, 10455−10462.

(74) Hajek, J.; Caratelli, C.; Demuynck, R.; De Wispelaere, K.; Vanduyfhuys, L.; Waroquier, M.; Van Speybroeck, V. On the intrinsic dynamic nature of the rigid UiO-66 metal−organic framework. *Chem. Sci.* **2018**, *9*, 2723−2732.

(75) Namsani, S.; Ozcan, A.; Yazaydın, A. Ö. Direct simulation of ternary mixture separation in a ZIF-8 membrane at molecular scale. *Adv. Theory Simul.* **2019**, *2*, 1900120.

(76) Heinen, J.; Dubbeldam, D. On flexible force fields for metal−organic frameworks: Recent developments and future prospects. *Wiley Interdiscip. Rev.: Comput. Mol. Sci.* **2018**, *8*, No. e1363.

(77) Forester, T. R.; Smith, W. Bluemoon simulations of benzene in silicalite-1 Prediction of free energies and diffusion coefficients. *J. Chem. Soc., Faraday Trans.* **1997**, *93*, 3249−3257.
(78) Kolokathis, P. D.; Káli, G.; Jobic, H.; Theodorou, D. N. Diffusion of aromatics in silicalite-1: Experimental and theoretical evidence of entropic barriers. *J. Phys. Chem. C* **2016**, *120*, 21410−21426.
(79) Nagumo, R.; Takaba, H.; Nakao, S.-i. Accelerated computation of extremely 'slow' molecular diffusivity in nanopores. *Chem. Phys. Lett.* **2008**, *458*, 281−284.
(80) Beerdsen, E.; Smit, B.; Dubbeldam, D. Molecular simulation of loading dependent slow diffusion in confined systems. *Phys. Rev. Lett.* **2004**, *93*, 248301.
(81) Poursaeidesfahani, A.; de Lange, M. F.; Khodadadian, F.; Dubbeldam, D.; Rigutto, M.; Nair, N.; Vlugt, T. J. H. Product shape selectivity of MFI-type, MEL-type, and BEA-type zeolites in the catalytic hydroconversion of heptane. *J. Catal.* **2017**, *353*, 54−62.
(82) Camp, J. S.; Sholl, D. S. Transition state theory methods to measure diffusion in flexible nanoporous materials: Application to a porous organic cage crystal. *J. Phys. Chem. C* **2016**, *120*, 1110−1120.
(83) Dubbeldam, D.; Beerdsen, E.; Vlugt, T. J. H.; Smit, B. Molecular simulation of loading-dependent diffusion in nanoporous materials using extended dynamically corrected transition state theory. *J. Chem. Phys.* **2005**, *122*, 224712.
(84) Dubbeldam, D.; Beerdsen, E.; Calero, S.; Smit, B. Dynamically corrected transition state theory calculations of self-diffusion in anisotropic nanoporous materials. *J. Phys. Chem. B* **2006**, *110*, 3164−3172.
(85) Smit, B.; Maesen, T. L. M. Towards a molecular understanding of shape selectivity. *Nature* **2008**, *451*, 671−678.
(86) Snurr, R. Q.; Bell, A. T.; Theodorou, D. N. Investigation of the dynamics of benzene in silicalite using Transition-State Theory. *J. Phys. Chem.* **1994**, *98*, 11948−11961.
(87) Kolokathis, P. D.; Pantatosaki, E.; Gatsiou, C.-A.; Jobic, H.; Papadopoulos, G. K.; Theodorou, D. N. Dimensionality reduction of free energy profiles of benzene in silicalite-1: calculation of diffusion coefficients using transition state theory. *Mol. Simul.* **2014**, *40*, 80−100.
(88) Kolokathis, P. D.; Braun, O. M. KoBra: A rate constant method for prediction of the diffusion of sorbates inside nanoporous materials at different loadings. *J. Comput. Chem.* **2019**, *40*, 2053−2066.
(89) Demontis, P.; Suffritti, G. B.; Quartieri, S.; Fois, E. S.; Gamba, A. Molecular dynamics studies on zeolites. II: A simple model for silicates applied to anhydrous natrolite. *Zeolites* **1987**, *7*, 522−527.
(90) Awati, R. V.; Ravikovitch, P. I.; Sholl, D. S. Efficient and accurate methods for characterizing effects of framework flexibility on molecular diffusion in zeolites: CH4 diffusion in eight member ring zeolites. *J. Phys. Chem. C* **2013**, *117*, 13462−13473.
(91) Awati, R. V.; Ravikovitch, P. I.; Sholl, D. S. Efficient calculation of gas diffusivity in single-component and binary mixtures of spherical adsorbates in flexible 8MR zeolites. *J. Phys. Chem. C* **2015**, *119*, 16596−16605.
(92) Gee, J. A.; Sholl, D. S. Effect of framework flexibility on C_8 aromatic adsorption at high loadings in metal−organic frameworks. *J. Phys. Chem. C* **2016**, *120*, 370−376.
(93) Poursaeidesfahani, A.; Torres-Knoop, A.; Dubbeldam, D.; Vlugt, T. J. H. Direct free energy calculation in the Continuous Fractional Component Gibbs ensemble. *J. Chem. Theory Comput.* **2016**, *12*, 1481−1490.
(94) Shi, W.; Maginn, E. J. Continuous Fractional Component Monte Carlo: An adaptive biasing method for open system atomistic simulations. *J. Chem. Theory Comput.* **2007**, *3*, 1451−1463.
(95) Dubbeldam, D.; Calero, S.; Ellis, D. E.; Snurr, R. Q. RASPA: molecular simulation software for adsorption and diffusion in flexible nanoporous materials. *Mol. Simul.* **2016**, *42*, 81−101.
(96) Dubbeldam, D.; Torres-Knoop, A.; Walton, K. S. On the inner workings of Monte Carlo codes. *Mol. Simul.* **2013**, *39*, 1253−1292.
(97) van Koningsveld, H.; van Bekkum, H.; Jansen, J. C. On the location and disorder of the tetrapropylammonium (TPA) ion in zeolite ZSM-5 with improved framework accuracy. *Acta Crystallogr., Sect. B: Struct. Sci.* **1987**, *43*, 127−132.
(98) Jablonka, K. M.; Ongari, D.; Smit, B. Applicability of tail corrections in the molecular simulations of porous materials. *J. Chem. Theory Comput.* **2019**, *15*, 5635−5641.
(99) Allen, M. P.; Tildesley, D. *Computer Simulation of Liquids*, 2nd ed.; Oxford University Press, 2017.
(100) Torres-Knoop, A.; Balaji, S. P.; Vlugt, T. J. H.; Dubbeldam, D. A comparison of advanced Monte Carlo methods for open systems: CFCMC vs CBMC. *J. Chem. Theory Comput.* **2014**, *10*, 942−952.
(101) Hens, R.; Rahbari, A.; Caro-Ortiz, S.; Dawass, N.; Erdős, M.; Poursaeidesfahani, A.; Salehi, H. S.; Celebi, A. T.; Ramdin, M.; Moultos, O. A.; Dubbeldam, D.; Vlugt, T. J. H. Brick-CFCMC: Open source software for Monte Carlo simulations of phase and reaction equilibria using the Continuous Fractional Component Method. *J. Chem. Inf. Model.* **2020**, *60*, 2678−2682.
(102) Mentzen, B. F.; Gelin, P. The silicalite/p-xylene system : Part I — Flexibility of the MFI framework and sorption mechanism observed during p-xylene pore-filling by X-ray powder diffraction at room temperature. *Mater. Res. Bull.* **1995**, *30*, 373−380.
(103) Gelb, L. D.; Gubbins, K. E. Pore size distributions in porous glasses: A computer simulation study. *Langmuir* **1999**, *15*, 305−308.
(104) Sarkisov, L.; Harrison, A. Computational structure characterisation tools in application to ordered and disordered porous materials. *Mol. Simul.* **2011**, *37*, 1248−1257.
(105) Widom, B. Some topics in the theory of fluids. *J. Chem. Phys.* **1963**, *39*, 2808−2812.
(106) Frenkel, D.; Smit, B. *Understanding Molecular Simulation*, 2nd ed.; Academic Press, 2002.
(107) Dubbeldam, D.; Calero, S.; Vlugt, T. J. H. iRASPA: GPU-accelerated visualization software for materials scientists. *Mol. Simul.* **2018**, *44*, 653−676.
(108) Bueno-Pérez, R.; Calero, S.; Dubbeldam, D.; Ania, C. O.; Parra, J. B.; Zaderenko, A. P.; Merkling, P. J. Zeolite force fields and experimental siliceous frameworks in a comparative infrared study. *J. Phys. Chem. C* **2012**, *116*, 25797−25805.
(109) Guo, J.; Hammond, K. D. Comparison of siliceous zeolite potentials from the perspective of infrared spectroscopy. *J. Phys. Chem. C* **2018**, *122*, 6093−6102.
(110) van Beest, B. W. H.; Kramer, G. J.; van Santen, R. A. Force fields for silicas and aluminophosphates based on ab initio calculations. *Phys. Rev. Lett.* **1990**, *64*, 1955−1958.
(111) Kramer, G. J.; Farragher, N. P.; van Beest, B. W. H.; van Santen, R. A. Interatomic force fields for silicas, aluminophosphates, and zeolites: Derivation based on ab initio calculations. *Phys. Rev. B: Condens. Matter Mater. Phys.* **1991**, *43*, 5068−5080.
(112) Hill, J.-R.; Sauer, J. Molecular mechanics potential for silica and zeolite catalysts based on ab initio calculations. 2. aluminosilicates. *J. Phys. Chem.* **1995**, *99*, 9536−9550.
(113) Demontis, P.; Suffritti, G. B.; Quartieri, S.; Fois, E. S.; Gamba, A. Molecular dynamics studies on zeolites. 3. Dehydrated zeolite A. *J. Phys. Chem.* **1988**, *92*, 867−871.
(114) Demontis, P.; Suffritti, G. B.; Fois, E. S.; Gamba, A.; Morosi, G. A potential for molecular dynamics simulations of structural and dynamic properties of hydrate aluminosilicates. *Mater. Chem. Phys.* **1991**, *29*, 357−367.
(115) Nicholas, J. B.; Hopfinger, A. J.; Trouw, F. R.; Iton, L. E. Molecular modeling of zeolite structure. 2. Structure and dynamics of silica sodalite and silicate force field. *J. Am. Chem. Soc.* **1991**, *113*, 4792−4800.
(116) Gabrieli, A.; Sant, M.; Demontis, P.; Suffritti, G. B. Development and optimization of a new force field for flexible aluminosilicates, enabling fast molecular dynamics simulations on parallel architectures. *J. Phys. Chem. C* **2013**, *117*, 503−509.
(117) Ghysels, A.; Moors, S. L. C.; Hemelsoet, K.; De Wispelaere, K.; Waroquier, M.; Sastre, G.; Van Speybroeck, V. Shape-selective diffusion of olefins in 8-ring solid acid microporous zeolites. *J. Phys. Chem. C* **2015**, *119*, 23721−23734.

(118) Sastre, G.; Kärger, J.; Ruthven, D. M. Molecular dynamics study of diffusion and surface permeation of benzene in silicalite. *J. Phys. Chem. C* **2018**, *122*, 7217−7225.
(119) Bai, P.; Tsapatsis, M.; Siepmann, J. I. TraPPE-zeo: Transferable potentials for phase equilibria force field for all-silica zeolites. *J. Phys. Chem. C* **2013**, *117*, 24375−24387.
(120) Caro-Ortiz, S.; Hens, R.; Zuidema, E.; Rigutto, M.; Dubbeldam, D.; Vlugt, T. J. H. Molecular simulation of the vapor-liquid equilibria of xylene mixtures: Force field performance, and Wolf vs. Ewald for electrostatic interactions. *Fluid Phase Equilib.* **2019**, *485*, 239−247.
(121) Caro-Ortiz, S.; Hens, R.; Zuidema, E.; Rigutto, M.; Dubbeldam, D.; Vlugt, T. J. H. Corrigendum to "Molecular simulation of the vapor-liquid equilibria of xylene mixtures: Force field performance, and Wolf vs. Ewald for electrostatic Interactions" [Fluid Phase Equilib.] 485 (2019) 239−247. *Fluid Phase Equilib.* **2020**, *506*, 112370.
(122) Rai, N.; Siepmann, J. I. Transferable potentials for phase equilibria. 9. Explicit hydrogen description of benzene and five-membered and six-membered heterocyclic aromatic compounds. *J. Phys. Chem. B* **2007**, *111*, 10790−10799.
(123) Rai, N.; Siepmann, J. I. Transferable potentials for phase equilibria. 10. Explicit-hydrogen description of substituted benzenes and polycyclic aromatic compounds. *J. Phys. Chem. B* **2013**, *117*, 273−288.
(124) Bonnaud, P.; Nieto-Draghi, C.; Ungerer, P. Anisotropic united atom model including the electrostatic interactions of benzene. *J. Phys. Chem. B* **2007**, *111*, 3730−3741.
(125) Nieto-Draghi, C.; Bonnaud, P.; Ungerer, P. Anisotropic united atom model including the electrostatic interactions of methylbenzenes. I. Thermodynamic and structural properties. *J. Phys. Chem. C* **2007**, *111*, 15686−15699.
(126) Nieto-Draghi, C.; Bonnaud, P.; Ungerer, P. Anisotropic united atom model including the electrostatic interactions of methylbenzenes. II. Transport properties. *J. Phys. Chem. C* **2007**, *111*, 15942−15951.
(127) Jorgensen, W. L.; Laird, E. R.; Nguyen, T. B.; Tirado-Rives, J. Monte Carlo simulations of pure liquid substituted benzenes with OPLS potential functions. *J. Comput. Chem.* **1993**, *14*, 206−215.
(128) Jorgensen, W. L.; Maxwell, D. S.; Tirado-Rives, J. Development and testing of the OPLS all-atom force field on conformational energetics and properties of organic liquids. *J. Am. Chem. Soc.* **1996**, *118*, 11225−11236.
(129) Yin, D.; MacKerell, A. D., Jr. Combined ab initio/empirical approach for optimization of Lennard−Jones parameters. *J. Comput. Chem.* **1998**, *19*, 334−348.
(130) Cacelli, I.; Cinacchi, G.; Prampolini, G.; Tani, A. Computer simulation of solid and liquid benzene with an atomistic interaction potential derived from ab initio calculations. *J. Am. Chem. Soc.* **2004**, *126*, 14278−14286.
(131) Lopes, P. E. M.; Lamoureux, G.; Roux, B.; MacKerell, A. D. Polarizable empirical force field for aromatic compounds based on the classical Drude oscillator. *J. Phys. Chem. B* **2007**, *111*, 2873−2885.
(132) Sun, H. COMPASS: An ab initio force-field optimized for condensed-phase applications - Overview with details on alkane and benzene compounds. *J. Phys. Chem. B* **1998**, *102*, 7338−7364.
(133) Visscher, K. M.; Geerke, D. P. Deriving force-field parameters from first principles using a polarizable and higher order dispersion model. *J. Chem. Theory Comput.* **2019**, *15*, 1875−1883.
(134) Wick, C. D.; Martin, M. G.; Siepmann, J. I. Transferable potentials for phase equilibria. 4. United-atom description of linear and branched alkenes and alkylbenzenes. *J. Phys. Chem. B* **2000**, *104*, 8008−8016.

https://dx.doi.org/10.1021/acs.jpcc.0c08054
J. Phys. Chem. C 2020, 124, 24488−24499